



Kolonia Harbour, Pohnpei

Chapter 4

Federated States of Micronesia

The contributions of David Aranug, Johannes Berdon and Eden Skilling from the Federated States of Micronesia National Weather Service Office are gratefully acknowledged

Introduction

This chapter provides a brief description of the Federated States of Micronesia, its past and present climate as well as projections for the future. The climate observation network and the availability of atmospheric and oceanic data records are outlined. The annual mean climate, seasonal cycles and the influences of large-scale climate features such as the Intertropical Convergence Zone and patterns of climate variability (e.g. the El Niño-Southern Oscillation) are

analysed and discussed. Observed trends and analysis of air temperature, rainfall, extreme events, sea-surface temperature, ocean acidification and mean and extreme sea level are presented. Projections for air and sea-surface temperature, rainfall, sea level and ocean acidification for the 21st century are provided, as are projections for tropical cyclones, drought, extreme rainfall, and extreme temperature. These projections are presented along

with confidence levels based on expert judgement by Pacific Climate Change Science Program (PCCSP) scientists. The chapter concludes with summary tables of projections for eastern and western Federated States of Micronesia. Projections are provided in imperial units and metric units (Tables 4.4 and 4.5). Important background information, including an explanation of methods and models, is provided in Chapter 1. For definitions of other terms refer to the Glossary.

4.1 Climate Summary

4.1.1 Current Climate

- There is little seasonal variation in monthly mean maximum and minimum air temperatures, with less than 3°F (1.5°C) between the average hottest and coolest months. Sea-surface temperatures around the Federated States of Micronesia influence the seasonal variations in air temperature.
- The wet season occurs from May to September when the Intertropical Convergence Zone is strongest and furthest north.
- The West Pacific Monsoon affects rainfall in the western Federated States of Micronesia, bringing additional rain during the wet season.
- Warming trends are evident at Pohnpei and Yap in annual and seasonal mean air temperatures for the periods 1950–2009 and 1951–2009 respectively.

- Annual and seasonal rainfall trends for Pohnpei for the period 1950–2009 and Yap for the period 1951–2009 are not statistically significant.
- The sea-level rise measured by satellite altimeters since 1993 is over 0.39 inches (10 mm) per year.
- The main extreme events that occur in the Federated States of Micronesia are droughts, typhoons, storm waves, flooding and landslides.

4.1.2 Future Climate

Over the course of the 21st century:

- Surface air temperature and sea-surface temperature are projected to continue to increase (*very high* confidence).
- Annual and seasonal mean rainfall is projected to increase (*high* confidence).

- The intensity and frequency of days of extreme heat are projected to increase (*very high* confidence).
- The intensity and frequency of days of extreme rainfall are projected to increase (*high* confidence).
- The incidence of drought is projected to decrease (*moderate* confidence).
- Tropical cyclone numbers are projected to decline in the tropical North Pacific Ocean basin (0–15°N, 130°E–180°E) (*moderate* confidence).
- Ocean acidification is projected to continue (*very high* confidence).
- Mean sea-level rise is projected to continue (*very high* confidence).

4.2 Country Description

The Federated States of Micronesia is located in the western North Pacific Ocean between the equator and 12°N, stretching from 136°E to 168°E. The country consists of four states: Yap, Chuuk, Pohnpei and Kosrae, listed in sequence from west to east. Of the total 607 islands, some are relatively large and mountainous, while the rest consist of smaller islands, flat coral atolls and raised coralline islands. The total land area comprises 271 square miles (702 km²) and this contrasts with the size of the Exclusive Economic Zone which totals 1.15 million square miles (2.98 million km²) (Federated

States of Micronesia's First National Communication under the UNFCCC, 1997; Federated States of Micronesia Country Statistics, SOPAC, 2010).

In 2010 the estimated population of the Federated States of Micronesia was 111 364 (Federated States of Micronesia Country Statistics, SOPAC, 2010). The capital city is Palikir in the state of Pohnpei.

Economic activity consists primarily of subsistence farming and agriculture. The Federated States of Micronesia has few mineral deposits except for high-grade phosphate. While the

potential exists for a tourism industry, its development is restricted by the country's remote location, few air connections and limited facilities for tourists (Federated States of Micronesia's Pacific Adaptation to Climate Change, 2006). The extensive tuna resources of the Exclusive Economic Zone are mainly exploited by Distant Water Fishing Nations under licence agreements (Federated States of Micronesia's First National Communication under the UNFCCC, 1997).

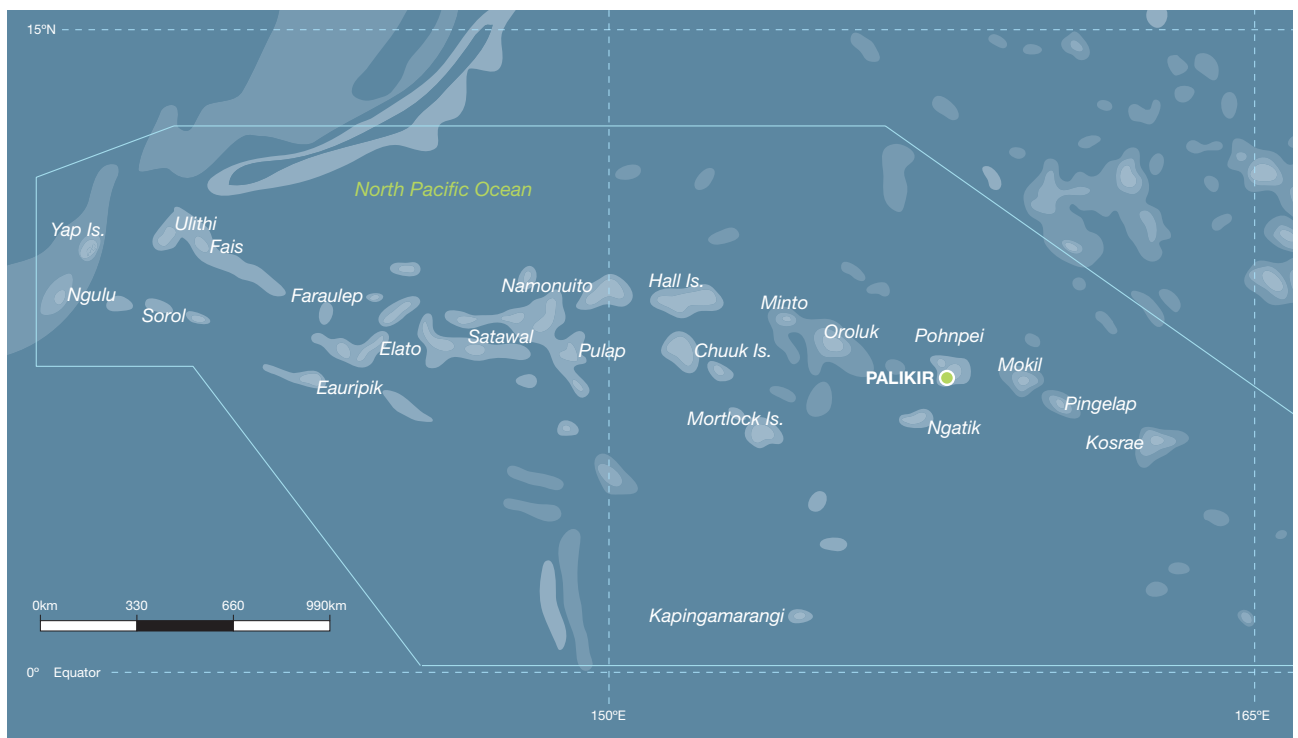


Figure 4.1: Federated States of Micronesia

4.3 Data Availability

There are 23 operational observation meteorological stations in the Federated States of Micronesia. Multiple observations within a 24-hour period are taken at five stations in Chuuk State, six in Pohnpei State (including Kosrae State) and three in Yap State. In addition, there are two single-observation-a-day climate stations in Pohnpei and seven single-observation-a-day rainfall stations in Yap (Figure 4.1).

Rainfall data for Pohnpei are available from 1949 and Yap from 1951. Air temperature data are available from 1950 for Pohnpei and 1951 for Yap. All available data from 1950 to 2009 are used. These records are homogeneous and more than 95% complete.

There are a number of sea-level records relevant for the Federated States of Micronesia. The best appear to be Guam (1948–present),

Yap (1969–2005), Chuuk (Moen Island, 1947–1995), Kapingamarangi (1978–2008), Pohnpei-B (1974–2004) and Pohnpei-C (2002–present). A global positioning system instrument to estimate vertical land motion was deployed at Pohnpei in 2003 and will provide valuable direct estimates of local vertical land motion in future years. Both satellite (from 1993) and in situ sea-level data (1950–2009; termed reconstructed sea level; Volume 1, Section 2.2.2.2) are available on a global 1° x 1° grid.

Long-term locally-monitored sea surface-temperature data are unavailable for the Federated States of Micronesia so large-scale gridded sea-surface temperature datasets have been used (HadISST, HadSST2, ERSST and Kaplan Extended SST V2; Volume 1, Table 2.3).



Training in *Pacific Climate Futures*

4.4 Seasonal Cycles

The seasonal variations in monthly mean maximum and minimum air temperatures are very small, with less than 3°F (1.5°C) between the average warmest and coolest months (Figure 4.2). In Pohnpei the highest average maximum air temperatures occur when average minimum air temperatures are lowest. However, in Yap average minimum air temperatures are extremely constant and maximum air temperatures are highest in April-May. As a country made up of small islands surrounded by ocean, seasonal variations in air temperatures are driven

by sea-surface temperatures around the Federated States of Micronesia.

The monthly mean rainfall cycle shows the distinction between the wet (May–October) and dry (November–April) seasons. The wet season occurs when the Intertropical Convergence Zone (ITCZ) is strongest and furthest north, closest to the Federated States of Micronesia. Pohnpei is close to the average position of the ITCZ, which is active year-round, so each month of the year Pohnpei's average rainfall is above

10 inches (250 mm). Rainfall is lower in Yap as it is further north. During the wet season in Yap there is a more noticeable presence of gusty winds and rainfall in association with the ITCZ. The West Pacific Monsoon (WPM) also affects rainfall in the Federated States of Micronesia, bringing additional rain during the wet season. This influence is strongest in Yap and other islands in the western Federated States of Micronesia and weaker in Pohnpei in the eastern side of the country.

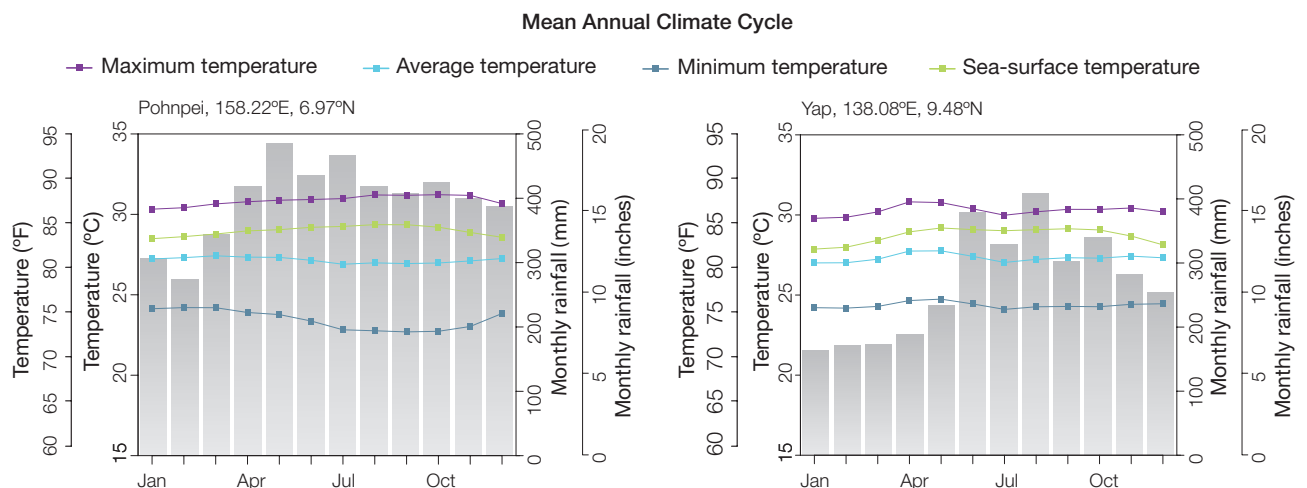


Figure 4.2: Mean annual cycle of rainfall (grey bars) and daily maximum, minimum and mean air temperatures at Pohnpei (left) and Yap (right), and local sea-surface temperatures derived from the HadISST dataset (Volume 1, Table 2.3).

4.5 Climate Variability

The El Niño-Southern Oscillation (ENSO) is the most important influence on the interannual climate variability in the Federated States of Micronesia (Figure 4.4 and correlation coefficients in Table 4.1). ENSO influences the minimum air temperatures in both Yap and Pohnpei in the wet season, but in the dry season there is a weak but significant impact on air minimum temperatures in Pohnpei and maximum air temperatures in Yap (all being warmer in El Niño years and colder in La Niña years).

During the driest years, Pohnpei and Yap receive about half the rainfall of the wettest years. The ENSO influence on rainfall is opposite in the two seasons in Pohnpei. In Yap the ENSO impact on rainfall is only significant in the dry season. In the dry season at both sites El Niño tends to result in drier conditions while La Niña tends to bring above average rainfall.

Although the influence is not as clear or as strong, El Niño brings higher than average rainfall during the wet season to Pohnpei. One mechanism by which this comes about is the position of the WPM. The monsoon tends to be farther east during El Niño, bringing higher wet season rainfall to Pohnpei, and in a more western position during La Niña, bringing lower rainfall. In Yap the ENSO impact is not significant in the wet season, so the WPM affects rainfall there in most years regardless of the phase of ENSO. The ITCZ brings less rainfall during El Niño events and more during La Niña. ENSO Modoki events (Volume1, Section 3.4.1) appear to have only a small effect, with only some weak but significant correlations on temperatures. ENSO Modoki events also have the same but weaker impact on Yap dry season rainfall as canonical ENSO events.

Table 4.1: Correlation coefficients between indices of key large-scale patterns of climate variability and minimum and maximum temperatures (Tmin and Tmax) and rainfall at Pohnpei. Only correlation coefficients that are statistically significant at the 95% level are shown.

| Climate feature/index | | Wet season (May-October) | | | Dry season (November-April) | | |
|--|----------------------------|-----------------------------|------|-------|--------------------------------|------|-------|
| | | Tmin | Tmax | Rain | Tmin | Tmax | Rain |
| ENSO | Niño3.4 | 0.26 | | 0.37 | 0.29 | | -0.68 |
| | Southern Oscillation Index | | | -0.33 | -0.31 | | 0.66 |
| Interdecadal Pacific Oscillation Index | | | | | | | |
| ENSO Modoki Index | | | | | 0.35 | | |
| Number of years of data | | 59 | 59 | 59 | 60 | 60 | 60 |

Table 4.2: Correlation coefficients between indices of key large-scale patterns of climate variability and minimum and maximum temperatures (Tmin and Tmax) and rainfall at Yap. Only correlation coefficients that are statistically significant at the 95% level are shown.

| Climate feature/index | | Wet season (May-October) | | | Dry season (November-April) | | |
|--|----------------------------|-----------------------------|------|------|--------------------------------|------|-------|
| | | Tmin | Tmax | Rain | Tmin | Tmax | Rain |
| ENSO | Niño3.4 | 0.49 | | | | 0.29 | -0.69 |
| | Southern Oscillation Index | -0.41 | | | | | 0.63 |
| Interdecadal Pacific Oscillation Index | | | | | | | |
| ENSO Modoki Index | | 0.31 | | | | | -0.32 |
| Number of years of data | | 58 | 58 | 58 | 59 | 59 | 59 |

4.6 Observed Trends

4.6.1 Air Temperature

Trends for seasonal and annual mean air temperatures at both Pohnpei (1950–2009) and Yap (1951–2009) are positive (Figure 4.3 and Table 4.3). The strongest trend is seen in Pohnpei in wet season (May–October) mean air temperatures (+0.24°C per decade). At Pohnpei, annual and seasonal trends in minimum air temperature are greater than those observed in maximum air temperature. However, at Yap, the trends in maximum air temperature in annual and dry season (November–April) records are much greater than those observed in minimum air temperatures.

4.6.2 Rainfall

Annual and seasonal rainfall trends for Pohnpei for the period 1950–2009 and Yap for the period 1951–2009 are not statistically significant (Table 4.3 and Figure 4.4).

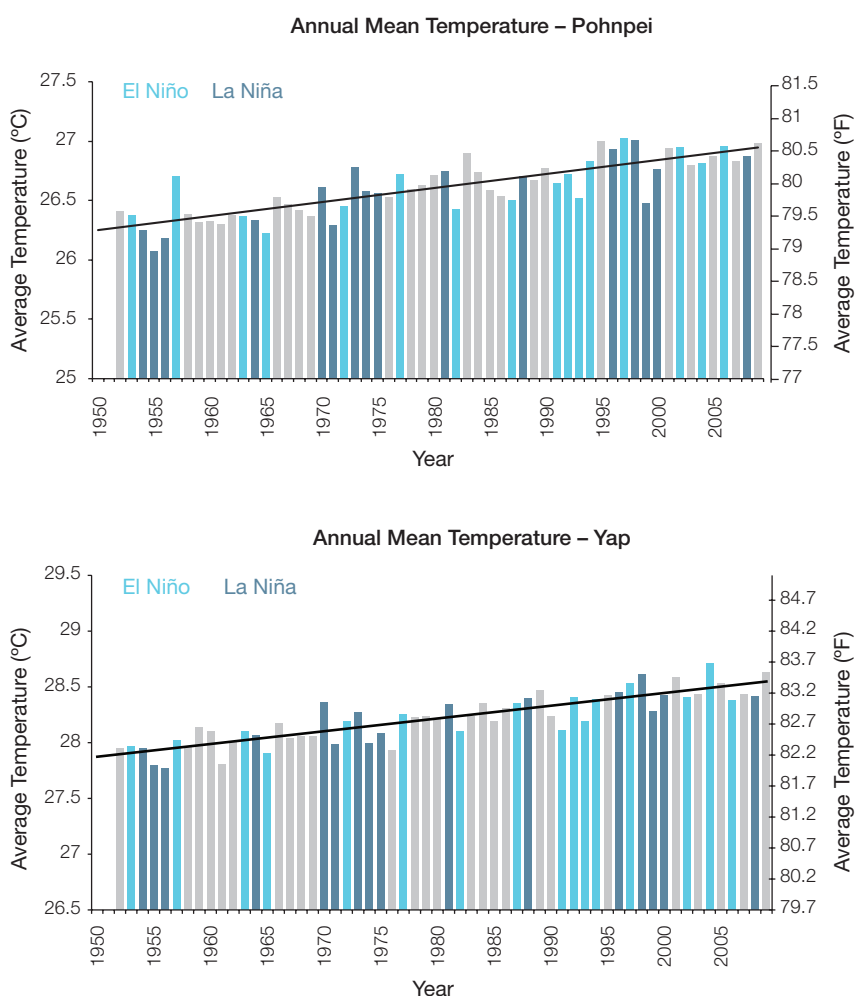


Figure 4.3: Annual mean air temperature in Pohnpei (top) and Yap (bottom). Light blue, dark blue and grey bars denote El Niño, La Niña and neutral years respectively.

Table 4.3: Annual and seasonal trends in maximum, minimum and mean air temperature (Tmax, Tmin and Tmean) and rainfall at Pohnpei for the period 1950–2009 and Yap for the period 1951–2009. Asterisks indicate significance at the 95% level. Persistence is taken into account in the assessment of significance as in Power and Kociuba (in press). The statistical significance of the air temperature trends is not assessed.

| | Pohnpei Tmax | Pohnpei Tmin | Pohnpei Tmean | Pohnpei Rain | Yap Tmax | Yap Tmin | Yap Tmean | Yap Rain |
|-------------------|-------------------------------------|-------------------------------------|-------------------------------------|--|-------------------------------------|-------------------------------------|-------------------------------------|--|
| | °F per 10 yrs (°C per 10 yrs) | °F per 10 yrs (°C per 10 yrs) | °F per 10 yrs (°C per 10 yrs) | inches per 10 yrs (mm per 10 yrs) | °F per 10 yrs (°C per 10 yrs) | °F per 10 yrs (°C per 10 yrs) | °F per 10 yrs (°C per 10 yrs) | inches per 10 yrs (mm per 10 yrs) |
| Annual | +0.19 (+0.11) | +0.24 (+0.13) | +0.21 (+0.12) | -2.7 (-68) | +0.24 (+0.13) | +0.18 (+0.10) | +0.21 (+0.11) | -0.1 (-3) |
| Wet season | +0.21 (+0.12) | +0.28 (+0.16) | +0.24 (+0.14) | -2.0 (-52) | +0.15 (+0.08) | +0.23 (+0.12) | +0.19 (+0.10) | +0.6 (+14) |
| Dry season | +0.17 (+0.10) | +0.19 (+0.10) | +0.18 (+0.10) | -1.0 (-26) | +0.32 (+0.18) | +0.13 (+0.07) | +0.22 (+0.12) | -0.6 (-15) |

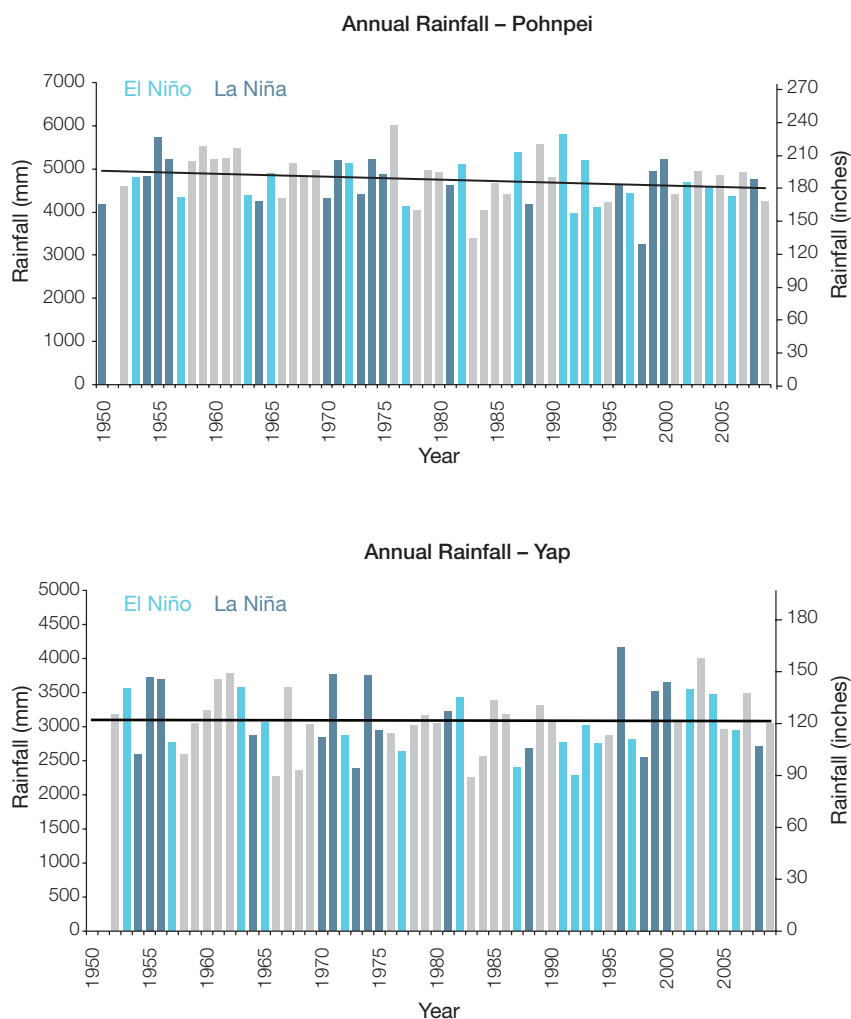


Figure 4.4: Annual rainfall in Pohnpei (top) and Yap (bottom). Light blue, dark blue and grey bars denote El Niño, La Niña and neutral years respectively.

4.6.3 Extreme Events

The main extreme events that occur in the Federated States of Micronesia are droughts, typhoons, storm waves, flooding and landslides. El Niño events are associated with less rainfall and occasionally droughts. These severe events have resulted in water and food shortages as well as the occurrence of fires. During La Niña events, above average numbers of tropical storms occur in the Federated States of Micronesia region.

On 2 July 2002, Tropical Storm Chataan struck the islands of Chuuk with 20 inches (~500 mm) of rainfall

received in a 24-hour period. Of the 265 landslides attributed to the storm, at least 62 massive landslides occurred on 2 July, resulting in 43 deaths and hundreds of injuries on six islands.

4.6.4 Sea-Surface Temperature

Historical changes around the Federated States of Micronesia are consistent with the broad-scale sea-surface temperature trends for the wider PCCSP region. Warming was relatively weak from the 1950s to the late 1980s. This was followed

by a period of more rapid warming (approximately 0.11°C per decade and approximately 0.08°C per decade for 1970–present, in the eastern and western regions respectively). At these regional scales, natural variability plays a large role in determining the sea-surface temperature, making it difficult to identify long-term trends.

4.6.5 Ocean Acidification

Based on the large-scale distribution of coral reefs across the Pacific and seawater chemistry, Guinotte et al. (2003) suggested that aragonite saturation states above 4 were optimal for coral growth and for the development of healthy reef ecosystems, with values from 3.5 to 4 adequate for coral growth, and values between 3 and 3.5, marginal. Coral reef ecosystems were not found at seawater aragonite saturation states below 3 and these conditions were classified as extremely marginal for supporting coral growth.

In the Federated States of Micronesia region, the aragonite saturation state has declined from about 4.5 in the late 18th century to an observed value of about 3.9 ± 0.1 by 2000.

4.6.6 Sea Level

Monthly averages of the historical tide gauge, satellite (since 1993) and gridded sea-level (since 1950) data agree well after 1993 and indicate interannual variability in sea levels of about 10 inches (26 cm) (estimated 5–95% range) after removal of the seasonal cycle (Figure 4.9). The sea-level rise near the Federated States of Micronesia measured by satellite altimeters (Figure 4.5) since 1993 is over 0.39 inches (10 mm) per year, larger than the global average of 0.125 ± 0.015 inches (3.2 ± 0.4 mm) per year. This rise is partly linked to a pattern related to climate variability from year to year and decade to decade (Figure 4.9).

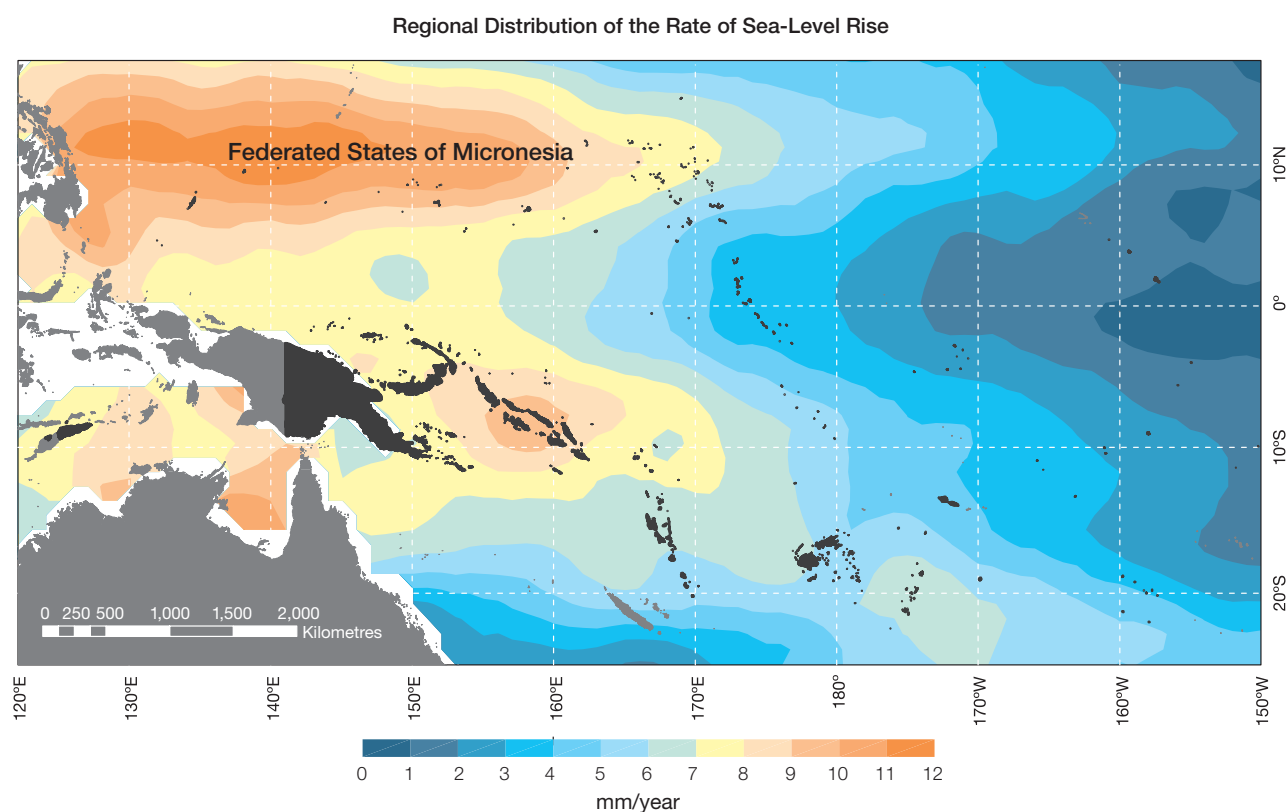


Figure 4.5: The regional distribution of the rate of sea-level rise measured by satellite altimeters from January 1993 to December 2010, with the location of the Federated States of Micronesia indicated. Further detail about the regional distribution of sea-level rise is provided in Volume 1, Section 3.6.3.2.

4.6.7 Extreme Sea-Level Events

The annual climatology of the highest daily sea levels has been evaluated from hourly measurements of tide gauges at Pohnpei and Chuuk (Figure 4.6). Highest tides at both locations tend to occur around the solstices, particularly at Chuuk, where there is a pronounced June maximum. These periods of highest tides lead to the maximum likelihood of high water levels at both locations in mid-April to

mid-July and November to January. Seasonal sea levels are significantly lower during El Niño conditions and significantly higher in La Niña conditions, approximately ± 0.49 ft (± 0.15 m) during October-February. This combination of high solstitial tides with seasonal water levels during October to February in La Niña years is supported by observations of the highest 10 recorded water levels at both sites of which seven of 10 occur during La Niña conditions, and eight occur between late October and

January at Pohnpei. None of highest 10 water levels at either location occurred during El Niño conditions. Chuuk, with its higher June tidal maximum, has a higher likelihood of extreme water levels during this month than Pohnpei. This tide gauge information indicates that most occurrences of extreme sea-level events at both Pohnpei and Chuuk are primarily due to a combination extreme tides and La Niña conditions.

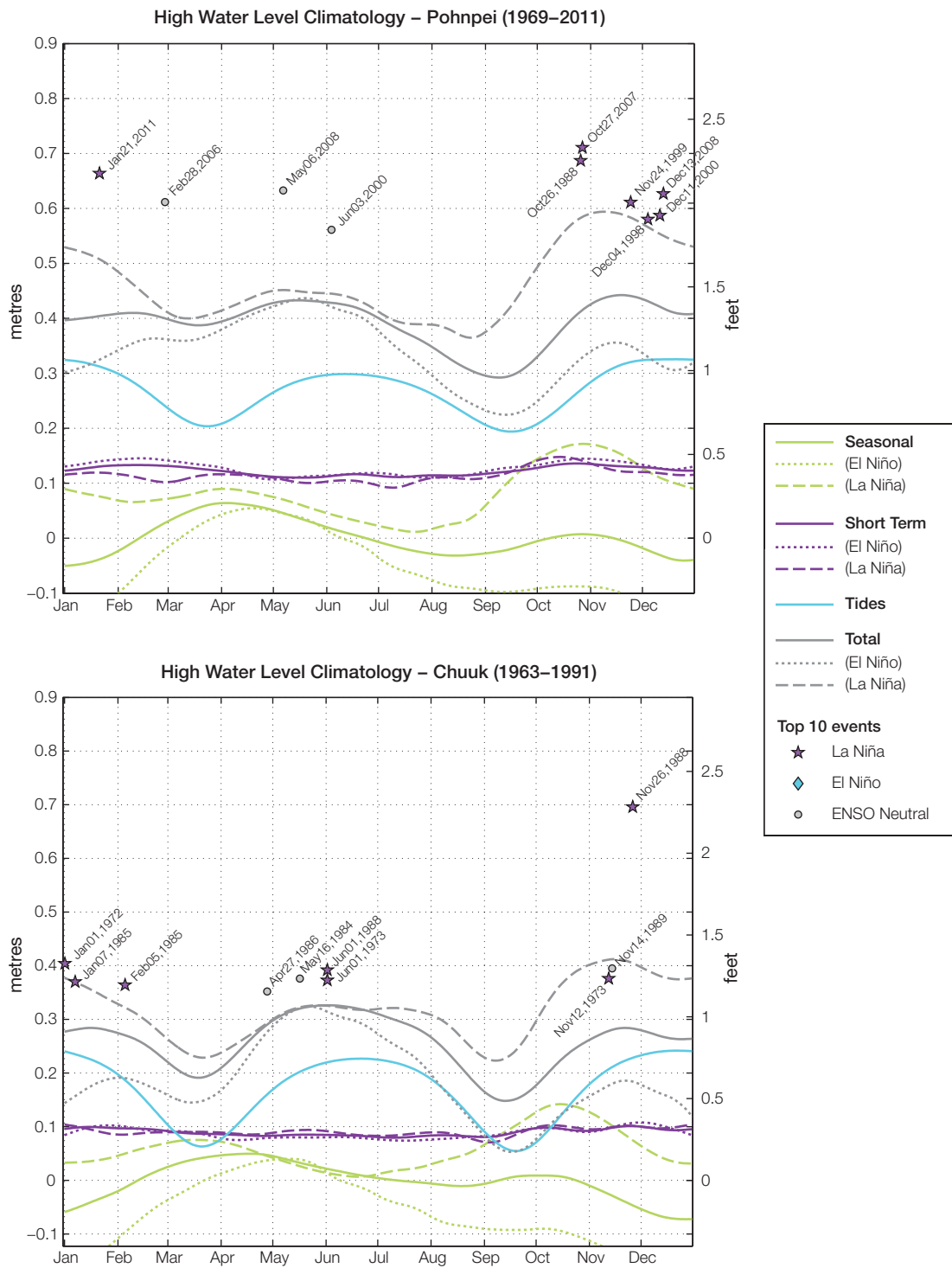


Figure 4.6: The annual cycle of high water levels relative to Mean Higher High Water (MHHW) due to tides, short-term fluctuations (most likely associated with storms) and seasonal variations for Pohnpei (top) and Chuuk (bottom). The tides and short-term fluctuations are respectively the 95% exceedence levels of the astronomical high tides relative to MHHW and short-term sea-level fluctuations. Components computed only for El Niño and La Niña years are shown by dotted and dashed lines, and grey lines are the sum of the tide, short-term and seasonal components. The 10 highest sea-level events in the record relative to MHHW are shown and coded to indicate the phase of ENSO at the time of the extreme event.

4.7 Climate Projections

Climate projections have been derived from up to 18 global climate models from the CMIP3 database, for up to three emissions scenarios (B1 (low), A1B (medium), A2 (high)) and three 20-year periods (centred on 2030, 2055 and 2090, relative to 1990) (Section 1.7.2). These models were selected based on their ability to reproduce important features of the current climate (Volume 1, Section 5.2.3), so projections arising from each of the models are a plausible representation of the future climate. This means there is not one single projected future for the Federated States of Micronesia, but rather a range of possible futures. The full range of these futures is discussed in the following sections.

These projections do not represent a value specific to any actual location, such as a town or city in the Federated States of Micronesia. Instead, they refer to an average change over the broad geographic region encompassing the islands of the Federated States of Micronesia and the surrounding ocean. Projections refer to the entire Federated States of Micronesia unless otherwise stated. In some instances, given there are some differences between the climate of the west (i.e. Yap and the western islands of Chuuk) and east (i.e. Kosrae, Pohnpei and the main island of Chuuk) (Section 4.4), the Federated States of Micronesia projections are given separately for these two regions (Figure 1.1 shows the regional boundaries). Some information regarding dynamical downscaling simulations from the CCAM model (Section 1.7.2) is also provided in order to indicate how changes in the climate on an individual island-scale may differ from the broad-scale average.

Section 1.7 provides important information about interpreting climate model projections.

4.7.1 Temperature

Surface air temperature and sea-surface temperature are projected to continue to increase over the course of the 21st century. There is *very high* confidence in this direction of change because:

- Warming is physically consistent with rising greenhouse gas concentrations.
- All CMIP3 models agree on this direction of change.

The majority of CMIP3 models simulate a slight increase (<1.8°F; <1°C) in annual and seasonal mean surface air temperature by 2030, however by 2090, under the A2 (high) emissions scenario, temperature increases of greater than 4.5°F (2.5°C) are simulated by almost all models (Tables 4.4 and 4.5). Given the close relationship between surface air temperature and sea-surface temperature, a similar (or slightly weaker) rate of warming is projected for the surface ocean (Figure 4.7). There is *high* confidence in this range and distribution of possible futures because:

- There is generally close agreement between modelled and observed temperature trends over the past 50 years in the vicinity of the Federated States of Micronesia, although observational records are limited (Figure 4.7).

The 8 km CCAM simulations did not resolve any spatial variability in the changes to surface air temperature. This result is partially a consequence of the Federated States of Micronesia still being poorly resolved even at 8 km resolution.

Interannual variability in sea-surface temperature and surface air temperature over the Federated States of Micronesia is strongly influenced by ENSO in the current climate (Section 4.5). As there is no consistency in projections of future ENSO activity

(Volume 1, Section 6.4.1), it is not possible to determine whether interannual variability in temperature will change in the future. However, ENSO is expected to continue to be an important source of variability for the Federated States of Micronesia and the region.

4.7.2 Rainfall

Wet season (May–October), dry season (November–April) and annual average rainfall is projected to increase over the course of the 21st century. There is *high* confidence in this direction of change because:

- Physical arguments indicate that rainfall will increase in the equatorial Pacific in a warmer climate (IPCC, 2007; Volume 1, Section 6.4.3).
- Almost all of the CMIP3 models agree on this direction of change by 2090.

The majority of CMIP3 models simulate little change (–5% to 5%) in rainfall by 2030, however by 2090 the majority simulate an increase (>5%) in wet season, dry season and annual rainfall, with up to a third simulating a large increase (>15%) for the eastern Federated States of Micronesia under the A2 (high) emissions scenario (Tables 4.4 and 4.5). There is *moderate* confidence in this range and distribution of possible futures because:

- In simulations of the current climate, the CMIP3 models broadly capture the influence of the West Pacific Monsoon and Intertropical Convergence Zone on the rainfall of the western and the entire Federated States of Micronesia regions respectively (Volume 1, Sections 5.2.3.4 and 5.2.3.5), although most models produce monsoon westerly winds that do not extend far enough east into the Pacific basin.

- The CMIP3 models are unable to resolve many of the physical processes involved in producing rainfall. As a consequence, they do not simulate rainfall as well as they simulate other variables such as temperature (Volume 1, Chapter 5).

The inconsistency between the projected increases in rainfall and the recent declining (Pohnpei) or relatively steady (Yap) trends observed at individual meteorological stations (Section 4.6.2) may be related to local factors not captured by the

models (e.g. topography), or the fact that the projections presented here represent an average over a very large geographic region (Sections 1.7.1 and 1.7.2).

Interannual variability in rainfall over the Federated States of Micronesia is strongly influenced by ENSO in the current climate (Section 4.5). As there is no consistency in projections of future ENSO activity (Volume 1, Section 6.4.1), it is not possible to determine whether interannual variability in rainfall will change in the future.

4.7.3 Extremes

Temperature

The intensity and frequency of days of extreme heat are projected to increase over the course of the 21st century. There is *very high* confidence in this direction of change because:

- An increase in the intensity and frequency of days of extreme heat is physically consistent with rising greenhouse gas concentrations.
- All CMIP3 models agree on the direction of change for both intensity and frequency.

For both the eastern and western Federated States of Micronesia, the majority of CMIP3 models simulate an increase of approximately 1.8°F (1°C) in the temperature experienced on the 1-in-20-year hot day by 2055 under the B1 (low) emissions scenario, with an increase of over 4.5°F (2.5°C) simulated by the majority of models by 2090 under the A2 (high) emissions scenario (Tables 4.4 and 4.5). There is *low* confidence in this range and distribution of possible futures because:

- In simulations of the current climate, the CMIP3 models tend to underestimate the intensity and frequency of days of extreme heat (Volume 1, Section 5.2.4).
- Smaller increases in the frequency of days of extreme heat are projected by the CCAM 60 km simulations.

Rainfall

The intensity and frequency of days of extreme rainfall are projected to increase over the course of the 21st century. There is *high* confidence in this direction of change because:

- An increase in the frequency and intensity of extreme rainfall is consistent with larger-scale projections, based on the physical argument that the atmosphere is able to hold more water vapour in a warmer climate (Allen and Ingram, 2002; IPCC, 2007). It is also consistent with physical arguments that rainfall will increase in the

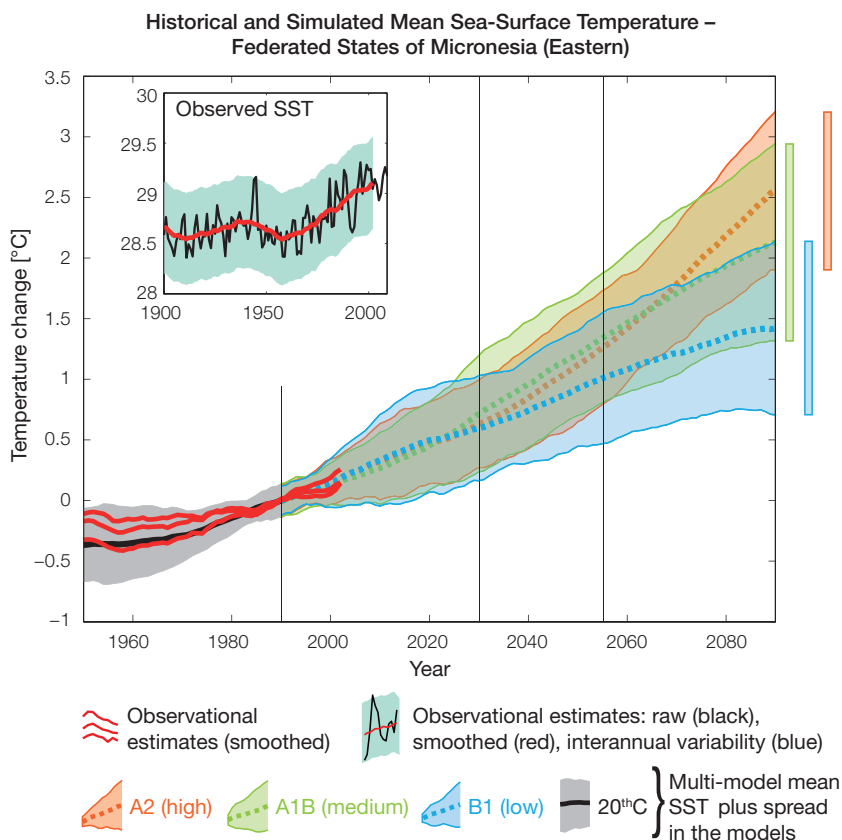


Figure 4.7: Historical climate (from 1950 onwards) and simulated historical and future climate for annual mean sea-surface temperature (SST) in the region surrounding the eastern Federated States of Micronesia for the CMIP3 models. Shading represents approximately 95% of the range of model projections (twice the inter-model standard deviation), while the solid lines represent the smoothed (20-year running average) multi-model mean temperature. Projections are calculated relative to the 1980–1999 period (which is why there is a decline in the inter-model standard deviation around 1990). Observational estimates in the main figure (red lines) are derived from the HadSST2, ERSST and Kaplan Extended SST V2 datasets (Volume 1, Section 2.2.2). Annual average (black) and 20-year running average (red) HadSST2 data is also shown inset. Projections for the western Federated States of Micronesia closely resemble those for the east and are therefore not shown.

deep tropical Pacific in a warmer climate (IPCC, 2007; Volume 1, Section 6.4.3).

- Almost all of the CMIP3 models agree on this direction of change for both intensity and frequency.

For both the eastern and western Federated States of Micronesia, the majority of CMIP3 models simulate an increase of at least 0.4 inches (10 mm) in the amount of rain received on the 1-in-20-year wet day by 2055 under a B1 (low) emissions scenario, with an increase of at least 0.8 inches (20 mm) simulated by all models by 2090 under the A2 (high) emissions scenario. The majority of models project that the current 1-in-20-year extreme rainfall event will occur, on average, two to three times every year by 2055 under the B1 (low) emissions scenario and five to six times every year by 2090 under the (A2) high emissions scenario. There is *low* confidence in this range and distribution of possible futures because:

- In simulations of the current climate, the CMIP3 models tend to underestimate the intensity and frequency of extreme rainfall (Volume 1, Section 5.2.4).
- The CMIP3 models are unable to resolve many of the physical processes involved in producing extreme rainfall.

Drought

The incidence of drought is projected to decrease over the course of the 21st century. There is *moderate* confidence in this direction of change because:

- A decrease in drought is consistent with projections of increased rainfall (Section 4.7.2).
- The majority of models agree on this direction of change for most drought categories.

For both the eastern and western Federated States of Micronesia, the majority of CMIP3 models project that mild drought will occur approximately eight to nine times every 20 years in 2030. This frequency is projected to

decrease to seven to eight times every 20 years by 2090 under the B1 (low) emissions scenario, and six to seven times under the A1B (medium) and A2 (high) scenarios. The frequency of moderate drought is projected to decrease from once to twice every 20 years in 2030, to once every 20 years in 2090 for all emissions scenarios, while the majority of CMIP3 models project that severe droughts will occur approximately once every 20 years across all time periods and scenarios. There is *low* confidence in this range and distribution of possible futures because:

- There is only moderate confidence in the range of rainfall projections (Section 4.7.2), which directly influences projections of future drought conditions.

Tropical Cyclones (Typhoons)

Tropical cyclone numbers are projected to decline in the tropical North Pacific Ocean basin (0–15°S, 130°E–180°E) over the course of the 21st century. There is *moderate* confidence in this direction of change because:

- Many studies suggest a decline in tropical cyclone frequency globally (Knutson et al., 2010).
- Tropical cyclone numbers decline in the tropical North Pacific Ocean basin in the majority assessment techniques.

Based on the direct detection methodologies (Curvature Vorticity Parameter (CVP) and the CSIRO Direct Detection Scheme (CDD) described in Volume 1, Section 4.8.2), 80% of projections show no change or a decrease in tropical cyclone formation when applied to the CMIP3 climate models for which suitable output is available. When these techniques are applied to CCAM, 100% of projections show a decrease in tropical cyclone formation. In addition, the Genesis Potential Index (GPI) empirical technique suggests that conditions for tropical cyclone formation will become less favourable in the North Pacific Ocean basin, for the majority

(70%) of analysed CMIP3 models. There is *moderate* confidence in this range and distribution of possible futures because in simulations of the current climate, the CVP, CDD and GPI methods capture the frequency of tropical cyclone activity reasonably well (Volume 1, Section 5.4).

Consistent with this projected reduction in total cyclone numbers, five of the six 60 km CCAM simulations also show a decrease in the proportion of the most severe storms (those stronger than the current climate 90th percentile storm maximum wind speed). Most simulations project an increase in the proportion of storms occurring in the weaker categories. Associated with this is a reduction in cyclonic wind hazard.

4.7.4 Ocean Acidification

The acidification of the ocean will continue to increase over the course of the 21st century. There is *very high* confidence in this projection as the rate of ocean acidification is driven primarily by the increasing oceanic uptake of carbon dioxide, in response to rising atmospheric carbon dioxide concentrations.

Projections from all analysed CMIP3 models indicate that the annual maximum aragonite saturation state will reach values below 3.5 by about 2030 and continue to decline thereafter (Figure 4.8; Tables 4.4 and 4.5). There is *moderate* confidence in this range and distribution of possible futures because the projections are based on climate models without an explicit representation of the carbon cycle and with relatively low resolution and known regional biases.

The impact of acidification change on the health of reef ecosystems is likely to be compounded by other stressors including coral bleaching, storm damage and fishing pressure.

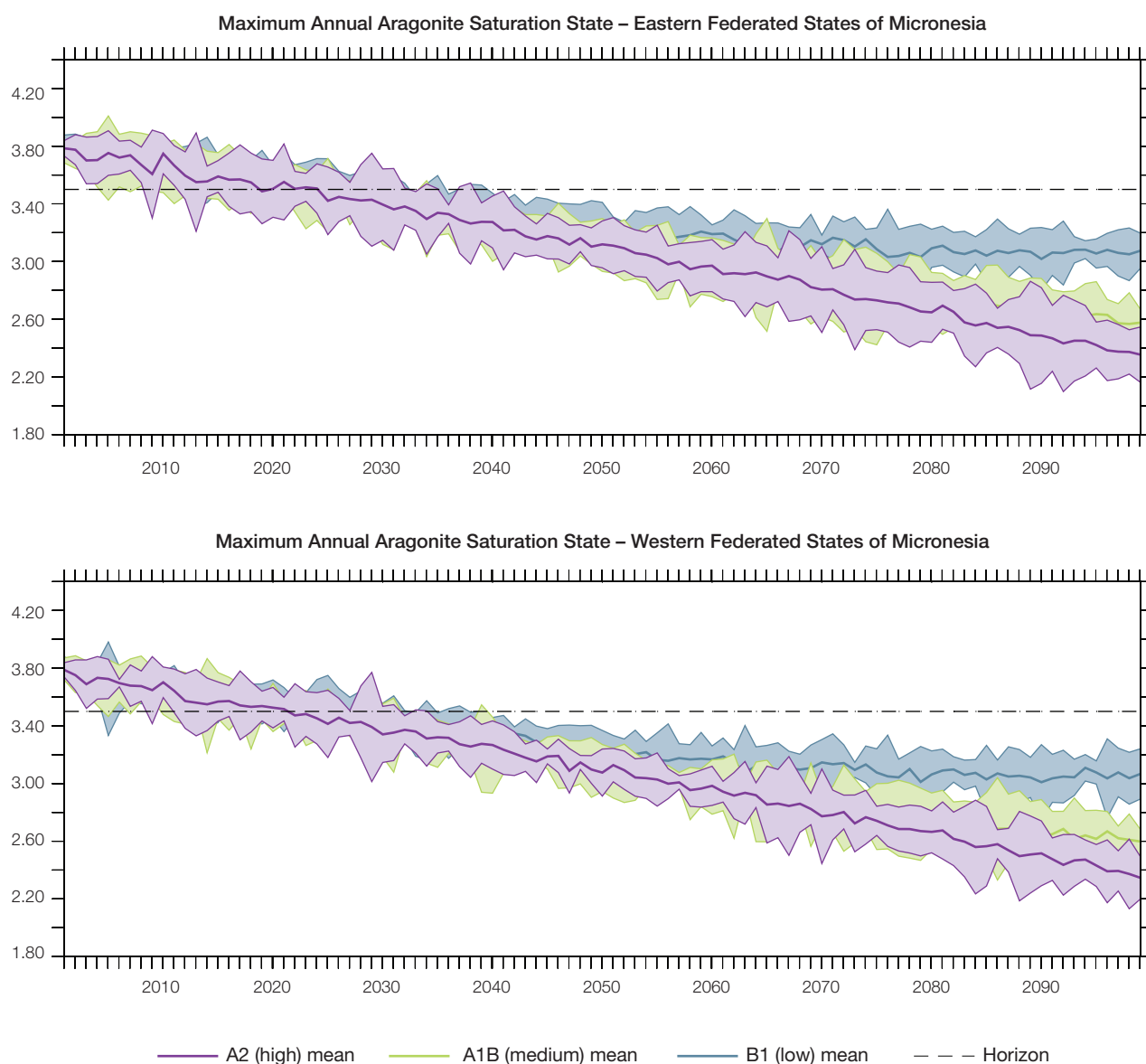


Figure 4.8: Multi-model projections, and their associated uncertainty (shaded area represents two standard deviations), of the maximum annual aragonite saturation state in the sea surface waters of the eastern Federated States of Micronesia (top) and the western Federated States of Micronesia (bottom) under the different emissions scenarios. The dashed black line represents an aragonite saturation state of 3.5.

4.7.5 Sea Level

Mean sea-level is projected to continue to rise over the course of the 21st century. There is *very high* confidence in this direction of change because:

- Sea-level rise is a physically consistent response to increasing ocean and atmospheric temperatures, due to thermal expansion and the melting of glaciers and ice caps.
- Projections arising from all CMIP3 models agree on this direction of change.

The CMIP3 models simulate a rise of between approximately 2–6 inches (5–15 cm) by 2030, with increases of 8–24 inches (20–60 cm) indicated by 2090 under the higher emissions scenarios (i.e. A1B (medium) and A2 (high); Figure 4.9; Tables 4.4 and 4.5). There is *moderate* confidence in this range and distribution of possible futures because:

- There is significant uncertainty surrounding ice-sheet contributions to sea-level rise and a larger rise than that projected above cannot be excluded (Meehl et al., 2007b). However, understanding of the processes is currently too limited to provide a best estimate or an upper bound (IPCC, 2007).

- Globally, since the early 1990s, sea level has been rising near the upper end of the above projections. During the 21st century, some studies (using semi-empirical models) project faster rates of sea-level rise.

Interannual variability of sea level will lead to periods of lower and higher regional sea levels. In the past, this interannual variability has been about 10 inches (26 cm) (5–95% range, after removal of the seasonal signal; dashed lines in Figure 4.9 (a)) and it is likely that a similar range will continue through the 21st century. In addition, winds and waves associated with weather phenomena will continue to lead to extreme sea-level events.

In addition to the regional variations in sea level associated with ocean and mass changes, there are ongoing changes in relative sea level associated with changes in surface loading over the last glacial cycle (glacial isostatic adjustment) and local tectonic motions. The glacial isostatic motions are relatively small for the PCCSP region.

4.7.6 Projections Summary

The projections presented in Section 4.7 are summarised in Table 4.4 (eastern Federated States of Micronesia) and Table 4.5 (western Federated States of Micronesia). Projections are presented in imperial and metric units. For detailed information regarding the various uncertainties associated with the table values, refer to the preceding text in Sections 4.7 and 1.7, in addition to Chapters 5 and 6 in Volume 1. When interpreting the differences between projections for the B1 (low), A1B (medium) and A2 (high) emissions scenarios, it is also important to consider the emissions pathways associated with each scenario (Volume 1, Figure 4.1) and the fact that a slightly different subset of models was available for each (Volume 1, Appendix 1).

Observed and Projected Relative Sea-Level Change Near the Federated States of Micronesia

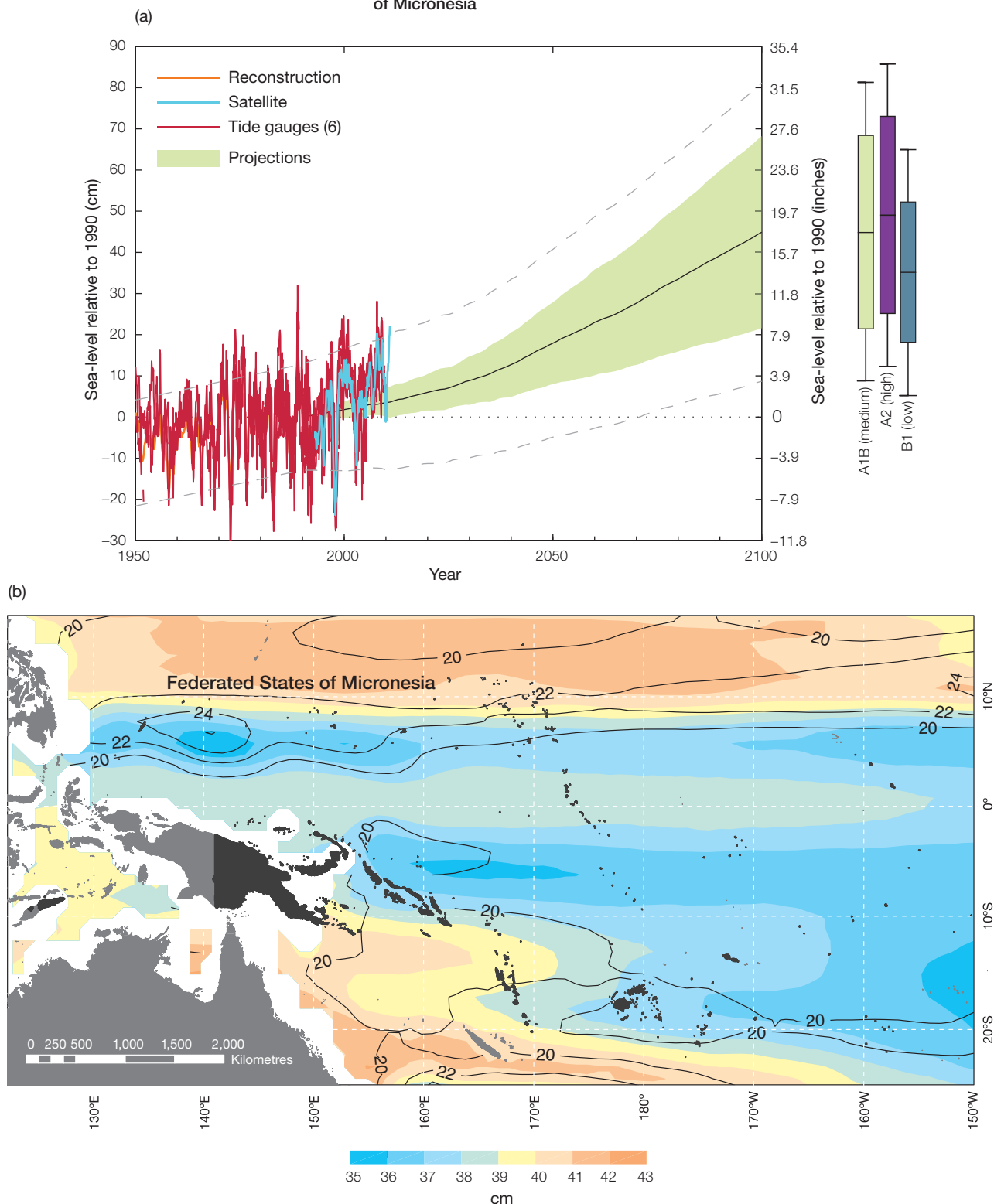


Figure 4.9: Observed and projected relative sea-level change near the Federated States of Micronesia. (a) The average of the observed in situ relative sea-level records is indicated in red, with the satellite record (since 1993) in light blue. The gridded sea-level data at the Federated States of Micronesia (since 1950, from Church and White (in press)) is shown in orange. The projections for the A1B (medium) emissions scenario (5–95% uncertainty range) are shown by the green shaded region from 1990–2100. The range of projections for the B1 (low), A1B (medium) and A2 (high) emissions scenarios by 2100 are also shown by the bars on the right. The dashed lines are an estimate of interannual variability in sea level (5–95% range about the long-term trends) and indicate that individual monthly averages of sea level can be above or below longer-term averages. (b) The projections (in cm) for the A1B (medium) emissions scenario in the Federated States of Micronesia region for the average over 2081–2100 relative to 1981–2000 are indicated by the shading, with the estimated uncertainty in the projections indicated by the contours (in cm).

Table 4.4: Projected change in the annual and seasonal mean climate for the eastern Federated States of Micronesia under the B1 (low; blue), medium A1B (medium; green) and A2 (high; purple) emissions scenarios. Projections are given for three 20-year periods centred on 2030 (2020–2039), 2055 (2046–2065) and 2090 (2080–2099), relative to 1990 (1980–1999). Values represent the multi-model mean change \pm twice the inter-model standard deviation (representing approximately 95% of the range of model projections), except for sea level where the estimated mean change and the 5–95% range are given (as they are derived directly from the Intergovernmental Panel on Climate Change Fourth Assessment Report values). The confidence (Section 1.7.2) associated with the range and distribution of the projections is also given (indicated by the standard deviation and multi-model mean, respectively). See Volume 1, Appendix 1 for a complete listing of CMIP3 models used to derive these projections.

| Variable | Season | 2030 | 2055 | 2090 | Confidence |
|--|--------------------|--|---|--|------------|
| Surface air temperature (°F) | Annual | +1.2 \pm 0.8 +1.4 \pm 0.9 +1.3 \pm 0.6 | +2.0 \pm 0.9 +2.7 \pm 1.1 +2.6 \pm 0.8 | +2.8 \pm 1.3 +4.3 \pm 1.6 +5.1 \pm 1.2 | High |
| Surface air temperature (°C) | Annual | +0.7 \pm 0.4 +0.8 \pm 0.5 +0.7 \pm 0.3 | +1.1 \pm 0.5 +1.5 \pm 0.6 +1.4 \pm 0.4 | +1.6 \pm 0.7 +2.4 \pm 0.9 +2.8 \pm 0.7 | High |
| Maximum temperature (°F) | 1-in-20-year event | N/A | +1.8 \pm 0.9 +2.5 \pm 1.1 +2.7 \pm 0.9 | +2.3 \pm 1.1 +3.8 \pm 1.8 +4.7 \pm 2.3 | Low |
| Maximum temperature (°C) | 1-in-20-year event | N/A | +1.0 \pm 0.5 +1.4 \pm 0.6 +1.5 \pm 0.5 | +1.3 \pm 0.6 +2.1 \pm 1.0 +2.6 \pm 1.3 | Low |
| Minimum temperature (°F) | 1-in-20-year event | N/A | +2.2 \pm 2.5 +2.7 \pm 2.7 +2.5 \pm 2.7 | +2.7 \pm 2.7 +3.8 \pm 3.2 +4.3 \pm 3.2 | Low |
| Minimum temperature (°C) | 1-in-20-year event | N/A | +1.2 \pm 1.4 +1.5 \pm 1.5 +1.4 \pm 1.5 | +1.5 \pm 1.5 +2.1 \pm 1.8 +2.4 \pm 1.8 | Low |
| Total rainfall (%)* | Annual | +1 \pm 8 +2 \pm 9 +4 \pm 11 | +7 \pm 8 +7 \pm 14 +7 \pm 11 | +7 \pm 11 +13 \pm 16 +12 \pm 15 | Moderate |
| Dry season rainfall (%)* | November-April | +1 \pm 15 +2 \pm 16 +4 \pm 14 | +7 \pm 9 +7 \pm 22 +8 \pm 18 | +7 \pm 12 +13 \pm 24 +10 \pm 19 | Moderate |
| Wet season rainfall (%)* | May-October | +2 \pm 10 +2 \pm 8 +4 \pm 12 | +7 \pm 12 +8 \pm 11 +7 \pm 13 | +8 \pm 14 +13 \pm 18 +14 \pm 21 | Moderate |
| Sea-surface temperature (°F) | Annual | +1.1 \pm 0.7 +1.3 \pm 0.9 +1.1 \pm 0.7 | +1.8 \pm 0.9 +2.3 \pm 0.9 +2.3 \pm 0.9 | +2.5 \pm 1.3 +3.8 \pm 1.4 +4.7 \pm 1.3 | High |
| Sea-surface temperature (°C) | Annual | +0.6 \pm 0.4 +0.7 \pm 0.5 +0.6 \pm 0.4 | +1.0 \pm 0.5 +1.3 \pm 0.5 +1.3 \pm 0.5 | +1.4 \pm 0.7 +2.1 \pm 0.8 +2.6 \pm 0.7 | High |
| Aragonite saturation state (Ω_{ar}) | Annual maximum | +3.4 \pm 0.1 +3.3 \pm 0.2 +3.4 \pm 0.2 | +3.2 \pm 0.1 +3.0 \pm 0.2 +3.0 \pm 0.2 | +3.0 \pm 0.1 +2.6 \pm 0.2 +2.4 \pm 0.2 | Moderate |
| Mean sea level (inches) | Annual | +3.5 (1.2–5.5) +3.5 (1.2–5.9) +3.5 (1.2–5.9) | +6.7 (3.5–10.2) +7.9 (3.5–12.6) +7.9 (3.9–11.8) | +12.2 (6.3–18.1) +15.4 (7.5–23.6) +16.1 (8.3–24.4) | Moderate |
| Mean sea level (cm) | Annual | +9 (3–14) +9 (3–15) +9 (3–15) | +17 (9–26) +20 (9–32) +20 (10–30) | +31 (16–46) +39 (19–60) +41 (21–62) | Moderate |

*The MIROC3.2(hires) model was eliminated in calculating the rainfall projections, due to its inability to accurately simulate present-day activity of the Intertropical Convergence Zone (Volume 1, Section 5.5.1).

Table 4.5: Projected change in the annual and seasonal mean climate for the western Federated States of Micronesia, under the B1 (low; blue), medium A1B (medium; green) and A2 (high; purple) emissions scenarios. Projections are given for three 20-year periods centred on 2030 (2020–2039), 2055 (2046–2065) and 2090 (2080–2099), relative to 1990 (1980–1999). Values represent the multi-model mean change \pm twice the inter-model standard deviation (representing approximately 95% of the range of model projections), except for sea level where the estimated mean change and the 5–95% range are given (as they are derived directly from the Intergovernmental Panel on Climate Change Fourth Assessment Report values). The confidence (Section 1.7.2) associated with the range and distribution of the projections is also given (indicated by the standard deviation and multi-model mean, respectively). See Volume 1, Appendix 1 for a complete listing of CMIP3 models used to derive these projections.

| Variable | Season | 2030 | 2055 | 2090 | Confidence |
|--|--------------------|--|---|--|------------|
| Surface air temperature (°F) | Annual | +1.1 \pm 0.7 +1.4 \pm 0.8 +1.3 \pm 0.5 | +1.9 \pm 0.9 +2.7 \pm 1.0 +2.5 \pm 0.8 | +2.7 \pm 1.3 +4.2 \pm 1.6 +5.0 \pm 1.2 | High |
| Surface air temperature (°C) | Annual | +0.6 \pm 0.4 +0.8 \pm 0.4 +0.7 \pm 0.3 | +1.0 \pm 0.5 +1.5 \pm 0.6 +1.4 \pm 0.4 | +1.5 \pm 0.7 +2.3 \pm 0.9 +2.8 \pm 0.7 | High |
| Maximum temperature (°F) | 1-in-20-year event | N/A | +1.8 \pm 0.7 +2.5 \pm 0.9 +2.7 \pm 1.1 | +2.3 \pm 1.3 +4.0 \pm 1.8 +4.9 \pm 2.3 | Low |
| Maximum temperature (°C) | 1-in-20-year event | N/A | +1.0 \pm 0.4 +1.4 \pm 0.5 +1.5 \pm 0.6 | +1.3 \pm 0.7 +2.2 \pm 1.0 +2.7 \pm 1.3 | Low |
| Minimum temperature (°F) | 1-in-20-year event | N/A | +2.3 \pm 2.9 +2.9 \pm 3.4 +2.5 \pm 2.9 | +3.1 \pm 2.9 +4.1 \pm 3.4 +4.7 \pm 3.6 | Low |
| Minimum temperature (°C) | 1-in-20-year event | N/A | +1.3 \pm 1.6 +1.6 \pm 1.9 +1.4 \pm 1.6 | +1.7 \pm 1.6 +2.3 \pm 1.9 +2.6 \pm 2.0 | Low |
| Total rainfall (%)* | Annual | 0 \pm 8 +1 \pm 7 +2 \pm 7 | +3 \pm 8 +5 \pm 15 +4 \pm 9 | +4 \pm 6 +9 \pm 15 +8 \pm 11 | Moderate |
| Dry season rainfall (%)* | November-April | 0 \pm 9 +1 \pm 9 +2 \pm 10 | +3 \pm 9 +6 \pm 21 +5 \pm 17 | +4 \pm 7 +9 \pm 20 +7 \pm 15 | Moderate |
| Wet season rainfall (%)* | May-October | +1 \pm 8 +1 \pm 7 +2 \pm 8 | +3 \pm 8 +5 \pm 11 +4 \pm 7 | +5 \pm 9 +9 \pm 14 +9 \pm 11 | Moderate |
| Sea-surface temperature (°F) | Annual | +1.1 \pm 0.9 +1.3 \pm 0.9 +1.3 \pm 0.7 | +2.0 \pm 1.1 +2.5 \pm 1.1 +2.3 \pm 0.9 | +2.7 \pm 1.4 +4.0 \pm 1.6 +4.7 \pm 1.3 | High |
| Sea-surface temperature (°C) | Annual | +0.6 \pm 0.5 +0.7 \pm 0.5 +0.7 \pm 0.4 | +1.1 \pm 0.6 +1.4 \pm 0.6 +1.3 \pm 0.5 | +1.5 \pm 0.8 +2.2 \pm 0.9 +2.6 \pm 0.7 | High |
| Aragonite saturation state (Ω_{ar}) | Annual maximum | +3.4 \pm 0.2 +3.3 \pm 0.1 +3.3 \pm 0.2 | +3.1 \pm 0.1 +3.0 \pm 0.2 +3.0 \pm 0.1 | +3.0 \pm 0.2 +2.6 \pm 0.2 +2.5 \pm 0.2 | Moderate |
| Mean sea level (inches) | Annual | +3.5 (1.2–5.5) +3.5 (1.2–5.9) +3.5 (1.2–5.9) | +6.7 (3.5–10.2) +7.9 (3.5–12.6) +7.9 (3.9–11.8) | +12.2 (6.3–18.1) +15.4 (7.5–23.6) +16.1 (8.3–24.4) | Moderate |
| Mean sea level (cm) | Annual | +9 (3–14) +9 (3–15) +9 (3–15) | +17 (9–26) +20 (9–32) +20 (10–30) | +31 (16–46) +39 (19–60) +41 (21–62) | Moderate |

*The MIROC3.2(medres) and MIROC3.2(hires) models were eliminated in calculating the rainfall projections, due to their inability to accurately simulate the West Pacific Monsoon and/or the Intertropical Convergence Zone (Volume 1, Section 5.5.1).